IEEE Photonics Journal
An IEEE Photonics Society Publication

Gain and Losses and Room-Temperature Operation in Interband Cascade Lasers

Volume 4, Number 1, February 2012

Geunmin Ryu, Member, IEEE
Athanasios N. Chryssis, Member, IEEE
Jeyran Amirloo, Member, IEEE
Simarjeet Saini, Member, IEEE
Fred J. Towner
Mario Dagenais, Fellow, IEEE

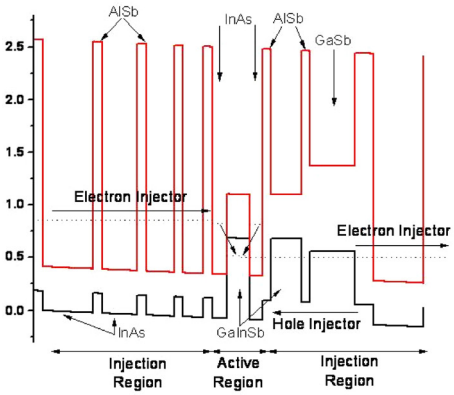

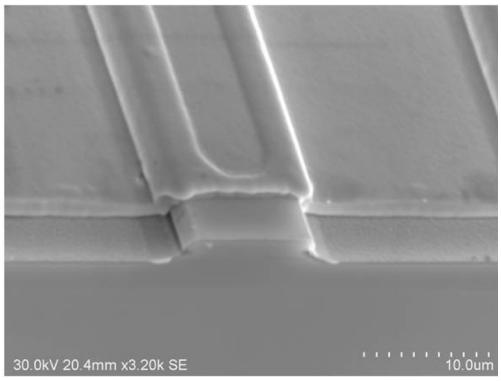

DOI: 10.1109/JPHOT.2011.2179640
1943-0655/$26.00 ©2011 IEEE

IEEE photonics SOCIETY

IEEE

Gain and Losses and Room-Temperature Operation in Interband Cascade Lasers

Geunmin Ryu,[1] *Member, IEEE*, Athanasios N. Chryssis,[1] *Member, IEEE*, Jeyran Amirloo,[1] *Member, IEEE*, Simarjeet Saini,[2] *Member, IEEE*, Fred J. Towner,[3] and Mario Dagenais,[1] *Fellow, IEEE*

[1]Department of Electrical and Computer Engineering, University of Maryland, College Park, MD 20742 USA
[2]Department of Electrical and Computer Engineering and Waterloo Institute of Nanotechnology, University of Waterloo, Waterloo, ON N2L 3G1 Canada
[3]Maxion Technologies, Inc., College Park, MD 20740 USA

DOI: 10.1109/JPHOT.2011.2179640

Manuscript received December 2, 2011; accepted December 3, 2011. Date of publication December 14, 2011; date of current version January 10, 2012. This work was supported by the National Aeronautics and Space Administration (NASA) under Contract NNX10CB61C as well as the encouragement and support provided by Dr. A. Yu and Dr. M. Krainak, both with NASA Goddard Space Flight Center, Greenbelt MD. The authors from the University of Maryland were supported by the Office of Naval Research sponsored the AppEl Center under Grant N000140911190 and by the Maryland NanoCenter and its FabLab. Corresponding author: M. Dagenais (e-mail: dage@eng.umd.edu).

Abstract: Interband cascade laser structures with a different number of cascades and doping types and levels in the separate confinement and in the hole-injection regions were grown. The temperature dependence of the gain and loss coefficients was measured. Although the gain dropped appreciably with increasing temperature, the internal losses remained nearly constant. Internal losses as low as 4.8 cm^{-1} were measured at room temperature in an optimized design. Internal quantum efficiency per cascade of 86% is achieved at 240 K. Room-temperature CW operation with a front facet output power of 42 mW was obtained in a 5-cascade structure with a 54% reduced size injection region. The laser operated at 3.8 μm.

Index Terms: Semiconductor laser, interband cascade laser (ICL), internal losses, quantum efficiency.

1. Introduction

Interband cascade lasers (ICLs) operate in the mid-infrared spectral region, in particular from 3 to 5 μm [1], [2]. They involve spatially indirect transitions between the conduction band in one semiconductor material and the valence band in a different semiconductor material in what has been referred to in the literature as a "W" type-II transition. In an ICL, each injected electron can cascade through several band-to-band transitions, and emit several photons. These lasers have demonstrated internal quantum efficiencies larger than 1. The ICLs are expected to play an important role in environmental monitoring, medical diagnostics, and infrared countermeasures. They have demonstrated very low threshold currents at cryogenic temperatures, as low as 4 A/cm^2. Unfortunately, because of the important role played by Auger recombination [3]–[5], the lasing threshold of these lasers increases dramatically as the operation temperature increases. Different approaches based on reducing the number of resonant paths for Auger recombination have been suggested for minimizing the role of Auger recombination in these lasers, but few convincing and systematic studies for achieving this have been conducted so far. Because of the high threshold

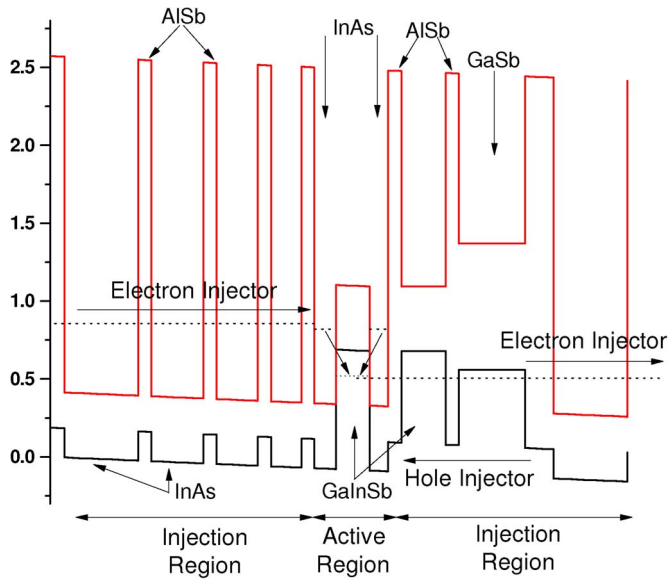

Fig. 1. Band structure of ICLs.

current densities and the associated high-energy dissipation, it has been difficult to operate these lasers cw at room temperature. Recently, by controlling the number of cascades, minimizing the absorption losses in these lasers, and improving the heat extraction, it has been possible to obtain room temperature operation but, arguably, only at low power [2], [6], [7]. A maximum power of 90 mW cw at 25 °C was demonstrated (total from front and back facet), with a wall-plug efficiency of 7.0%. There is a definite need to better understand both the role and how to control Auger recombination in these lasers. In addition, the temperature dependence of losses in these lasers, and how losses change as a function of the number of cascades, doping levels and type, optical confinement, width of the injection region, and the role of energy levels surrounding the active region have not been systematically studied. In our work, we have investigated different samples with different p- and n-doping levels in the separate confinement region (SCR), different number of cascades, different p-doping concentration of the hole injector near the active region, reduced width of the electron injector to increase the optical confinement. This leads to a better understanding of the impact of these parameters on the operation of ICLs. We have also studied the temperature dependence of the losses and of the gain coefficient. We have been able to obtain the lowest loss coefficient yet reported in these lasers. Our results clearly demonstrate that a reduction of the length of the injection region reduces the threshold current and increase the efficiency of these lasers. Also, we propose to increase the differential gain in these lasers by increasing the number of wells per cascade in the active region in order to make a more efficient laser.

2. Laser Layer Structure

Our lasers were grown by molecular beam epitaxy (MBE) on a p-type GaSb (001) substrate. They consist of five, six, or 12 interband cascaded stages. The lasing transition takes place in a "W" active region, whose type-II alignment with the next electron injector region allows electrons in the valence band to move back to the conduction band for transport into the next active stage. A representation of the active region with the electron and hole-injection regions is shown in Fig. 1.

The active region is composed of two electron InAs and one hole $Ga_{.7}In_{.3}Sb$ wells adjusted for emission around 3.5 μm. Since the electron injected into the InAs wells are effectively blocked from directly tunneling out, they recombine with holes in the $Ga_{.7}In_{.3}Sb$ quantum well (QW). The hole injector consists of a $Ga_{.7}In_{.3}Sb$ and a GaSb well. The electron injector structure is designed so

that, at the operating electric field, the QW states in adjacent InAs QWs are strongly coupled, forming a conduction miniband throughout the entire injection region. A smooth transport of electrons from each active region to the following one is realized. This cascading leads to sequential photon emission. The active/injection regions are surrounded by two separate GaSb confinement regions (SCRs) of 200 nm thickness. We have grown samples with either p- or n-doping in the SCR regions. A 4-μm n-type doped InAs/AlSb strained layer superlattice is used for the lower cladding, and a 1.4-μm n-type doped InAs/AlSb strained layer superlattice is used for the upper cladding. Finally, a heavily n-doped 10 nm thick InAs cap layer is used for contacting. Digitally graded InAs/AlInSb/AlSb transition regions are used between the SCRs and the cladding regions and from the clad to the substrate and to the cap layer to improve electron transport.

3. Characterization of 12 Cascades, p-Doped SCRs, ICLs

A 12-cascade ICL was grown by MBE according to the structure that was described in the previous section. In this ICL, the 200-nm-thick SCRs were p-doped at a concentration of 2.5×10^{17} cm^{-3}. Ridge lasers of 10 μm width were defined by contact lithography. A double trench structure was etched using a mixture of phosphoric acid, hydrogen peroxide, and tartaric acid. This structure maintains the planarity of the sample, allowing us to mount the device epi side down. We stopped the etch process in the lower optical superlattice cladding, just below the separate confinement layer (SCL). We then deposited a 400-nm-thick Si_3N_4 dielectric layer using plasma enhanced chemical vapor deposition (PECVD). Ti/Pt/Au contacts were evaporated by e-beam evaporator. The laser devices were cleaved in different lengths between 0.5- and 3-mm long devices. Devices with uncoated facets were mounted epi-up on AlN submounts using 3.5 μm of In solder. The AlN submount was then mounted on a copper heat sink with conducting epoxy. The Cu heat sinks were soldered to a TE cooler. In order to minimize the thermal effects, low duty cycle (1 kHz) 200 ns current pulses were used to drive the lasers. By varying the pulse duration from 200 ns to several microseconds, we observed that the slope efficiency of the lasers was very dependent on the pulse duration, in particular for lasers operated at room temperature. It was also observed that the threshold current density was less sensitive as compared to the slope efficiency when the pulse duration was varied. The emission wavelength of the lasers was around 3.5 μm. The following expressions describe the dependence of the threshold current density J_{th} on cavity length L_{cav} and the inverse of the slope efficiency $1/S$ on L_{cav} [4]:

$$J_{\text{th}} = \frac{q}{\eta_i \tau}\left[n_t + \frac{\alpha_i}{\Gamma \frac{dg}{dn}} - \frac{\ln R}{L_{\text{cav}}\Gamma \frac{dg}{dn}}\right] \tag{1}$$

$$\frac{1}{\eta_d} = \frac{h\nu}{2q}\frac{1}{S} = \frac{1}{\eta_i} + \frac{1}{\eta_i \ln\frac{1}{R}}\alpha_i L_{\text{cav}}. \tag{2}$$

In these expressions, n_t describe the transparency current density, α_i is the internal laser loss coefficient, $\Gamma(dg/dn)$ is the modal differential gain, η_i is the total internal efficiency and is equal to the number of cascades N multiplied by the internal efficiency per cascade, η_d is the differential efficiency, S is the slope efficiency, h is the Planck constant, τ is the carrier lifetime, and υ is the emission frequency. In (1) and (2), η_i is assumed to be the same in both expression, although strictly speaking, η_i in (2) is a differential quantity measured above threshold and η_i in (1) is a below threshold quantity [8]. A simulation of the mode profile in the laser using a plane wave decomposition model allowed us to extract the facet reflection coefficient to be $R = 0.38$. Fig. 2 shows our measurement of the inverse of the slope efficiency of the laser versus the cavity length for four different laser lengths measured at $T = 240$ K. In these measurements, we made sure that pulse durations of about 200 ns did not lead to any measurable dependence of the slope efficiency by extending the pulse duration by a factor of 2 and observing no change to the slope efficiency.

From this measurement, we extract the internal quantum efficiency per cascade of $1/(.0966 * N) = 0.86$. From (2), by taking the ratio of the slope to the intercept and multiplying the result by $\ln(1/R)$, we extract that the internal loss is 14.5 cm^{-1}. The uncertainty on this value is

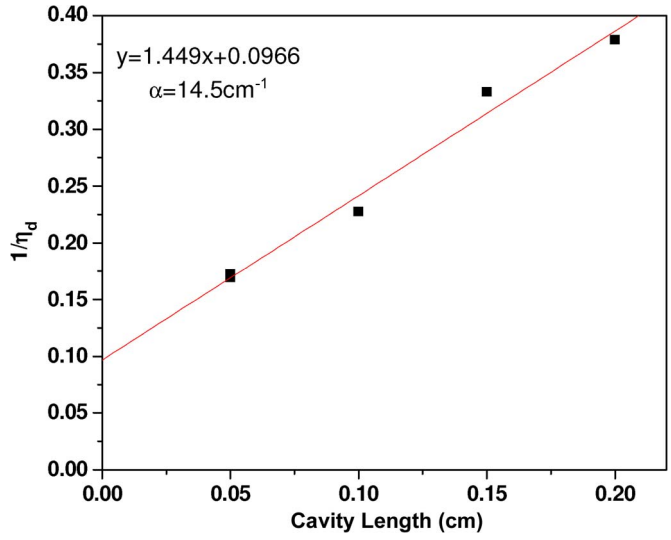

Fig. 2. 1/Differential efficiency versus Cavity length measured at $T = 240$ K.

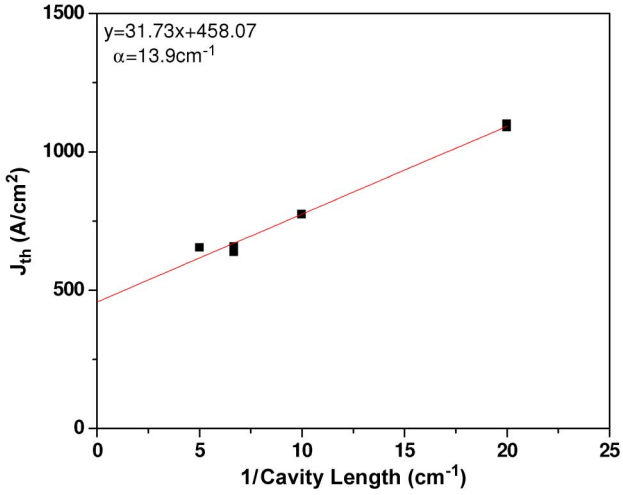

Fig. 3. J_{th} versus 1/Cavity length @ -33 °C for 12 cascade ICL with p-doped SCR.

extracted to be 1.0 cm^{-1}, based on a least square fit to the data. For the same sample, we also measured the threshold current density versus $1/L_{cav}$ at 240 K. The results are shown in Fig. 3. Using (1), dividing the ordinate by the slope and multiplying by $\ln(1/R)$, we extract that $n_t\ \Gamma(dg/dn) + \alpha_i = 13.9$ cm^{-1}. Comparing this result with the result obtained for the internal loss in the laser (14.5 cm^{-1}), we conclude that the transparency density term $n_t\ \Gamma(dg/dn)$ is much smaller than α_i and can be neglected. This is consistent with observations from another research team [4] who measured n_t at lower temperatures and found this term to be small. We do not expect that the relative size of these two terms will change significantly with temperature. In addition, we believe that the confinement factor (as we will see) is smaller in our sample, as compared with this other group, reducing even further the size of the n_t term. By neglecting this term, we find that the threshold current measurement approach gives us a very similar value of α_i.

The advantage of measuring the internal loss using the threshold current is that this approach is much less sensitive to thermal effects as the temperature of the sample is increased up to room temperature. We used the slope of the $L-I$ curve to extract the threshold current. Figs. 4 and 5

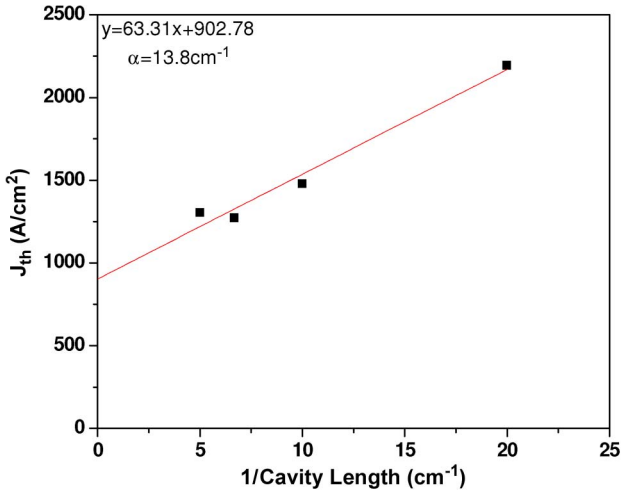

Fig. 4. J_{th} versus 1/Cavity length @ -0.4 °C for 12 cascade ICL with p-doped SCR.

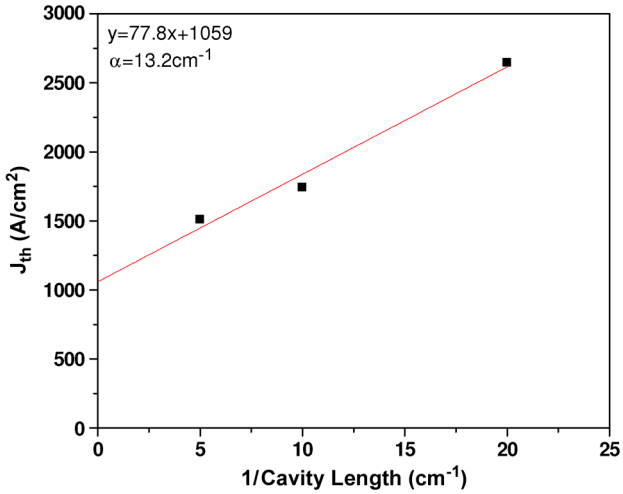

Fig. 5. J_{th} versus 1/Cavity length @ 7.7 °C for 12 cascade ICL with p-doped SCR.

show plots of J_{th} versus $1/L_{cav}$ at $T = 273.7$ and $T = 281$ K. Neglecting the n_t term, we extract that the internal loss in the laser at $T = 273.7$, and $T = 281$ K is 13.8 cm^{-1} and 13.2 cm^{-1}, respectively. Comparing these results with the $T = 240$ K results, we conclude that the internal loss coefficient is mostly temperature independent over the temperature range that was studied.

These results are in sharp contrast to previous results [1], [4], [9] which indicated a strong temperature dependence of the internal loss over the same temperature range. These other reported results were obtained using slope efficiency measurements, which are more susceptible to temperature effects and therefore less reliable.

From (1), we can extract the gain per unit current density at threshold, $G_J = (1/q)\eta_i\tau\Gamma(dG/dN)$, by taking the inverse of the measured slope of J_{th} versus $1/L_{cav}$ and multiplying by $1/\ln(R)$. In Fig. 6, we plot the gain per unit current density at threshold as a function of temperature. We extract a characteristic temperature of $T_0 = 45$ °C and a threshold gain per unit current density of 0.00781 cm/A at room temperature. Our value of the threshold gain per unit current density is lower than the value of 0.011 cm/A measured at $T = 300$ K by another group [4] by about 30%. We suspect that this difference comes from a proportionally lower value of the confinement factor in

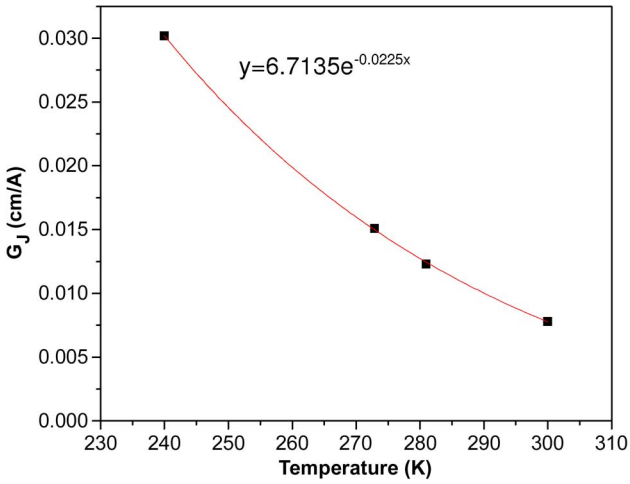

Fig. 6. Gain per unit current density versus Temperature for 12 cascade ICL with p-doped SCR.

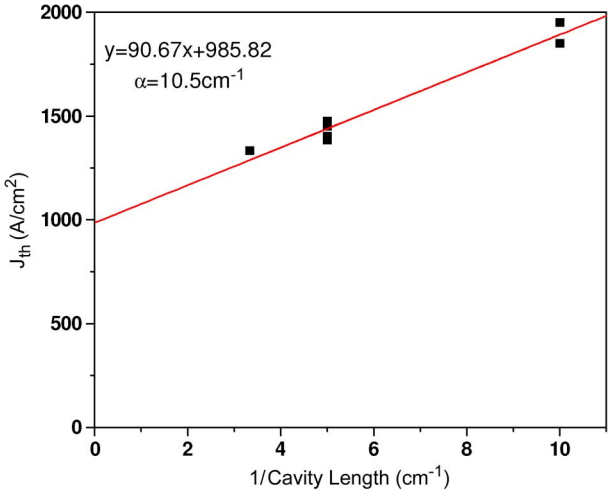

Fig. 7. J_{th} versus 1/Cavity length @*RT* for 12 cascade ICL with n-doped SCR.

our samples due to a possibly wider electron injection region. Unfortunately, we do not have access to the width of the electron injection region used in the NRL sample. The temperature dependence of G_J results from the temperature dependence of η_i, dG/dN, and τ. The carrier lifetime τ is strongly dependent on temperature because of the strong temperature dependence of Auger processes [10].

4. Characterization of 12 Cascades, n-Doped SCRs, ICLs

In order to assess the role of doping in the SCRs, another ICL was grown with two n-doped, 200-nm-thick SCRs. The doping concentration in the SCR was 2×10^{17} cm^{-3} and tellurium was used for n-doping. Apart from the change in the type of doping, the rest of the laser structure was identical to the 12-cascade ICL with p-doped SCR sample. This sample was also processed similarly. A plot of J_{th} versus $1/L_{cav}$ at room temperature is shown in Fig. 7. By taking the ratio of the ordinate to the slope and multiplying the result by $\ln(R)$, we extract an internal loss coefficient of 10.5 cm^{-1}. As expected, the internal loss is reduced by 3 cm^{-1} using n-type doping in the SCR. We attribute the 3 cm^{-1} loss coefficient to intervalence band absorption in the p-doped material, as it has been

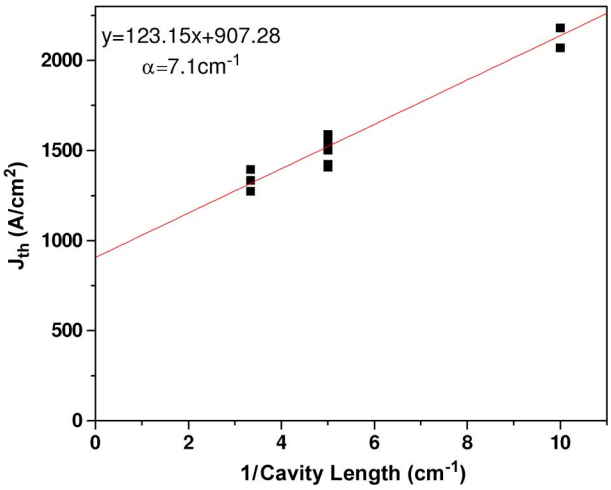

Fig. 8. J_{th} versus 1/Cavity length @*RT* for six cascade ICL with n-doped SCR.

reported to be the dominant absorption mechanism near 3.5 μm [11]. The absorption in n-doped material is believed to be due to intervalley conduction band absorption [11].

5. Characterization of Six Cascades, n-Doped SCRs, ICLs

In order to better understand how loss and gain vary as a function of the number of cascades, we grew a six-cascade ICL. The laser structure was identical to 12-cascade ICL with n-doped SCR sample, except that the number of cascades was reduced from 12 to six cascades. A measurement of J_{th} versus $1/L_{cav}$ at room temperature is shown in Fig. 8. By taking the ratio of the ordinate to the slope and multiplying the result by $\ln(R)$, we extract an absorption coefficient of 7.1 cm^{-1}. The internal loss coefficient is reduced by a factor of $10.5/7.1 = 1.47$ when going from 12 cascades to six cascades. The slope of J_{th} versus $1/L_{cav}$ is increased by $123/90.7 = 1.36$. A simulation of the mode size indicates that the confinement factor is reduced by a factor of 1.4 when the number of cascades is reduced from 12 to six cascades. Assuming that the differential gain per cascade dg/dn stays the same, we expect that the internal loss would decrease by the ratio of the confinement factors and we expect that the modal differential gain would increase by the same ratio, which is in good agreement with what is observed.

6. Characterization of Six Cascades, n-Doped SCRs, ICLs After Reduction of Losses in the Hole-Injection Region

A new six cascade, n-doped SCR, ICL was grown with the goal of further reducing losses in the active region. Since p-doping is used in the hole-injection region and since absorption is always larger for p-doped materials, we reduced the p-doping in both the GaInSb and the GaSb wells next to the active region. The p-doping in the GaInSb well was reduced from 0.7×10^{17} cm^{-3} to 0.4×10^{17} cm^{-3} and the p-doping in the GaSb well was reduced from 2.5×10^{17} to 1×10^{17} cm^{-3}. A measurement of J_{th} versus $1/L_{cav}$ at room temperature was performed in this sample and is shown in Fig. 9.

An internal loss coefficient of 4.8 cm^{-1} is extracted, a record low value for an ICL. The $\Gamma(dg/dn)$ factor appears to have also been reduced by a factor of 1.3, which might indicate that a p-doping reduction leads to a smaller extent of the wavefunction into the surrounding GaInSb well or to a reduction of the differential gain. A further reduction of the doping in the two surrounding wells (hole-injection layers) might lead to a further reduction of internal losses in the ICLs. Using this material, we demonstrated a significant improvement in the high-temperature operation of our ICLs compared with our previous best results of $T_{max} = 214$ K [12]. We have obtained a maximum cw temperature of operation of $T_{max} = 276$ K in this material.

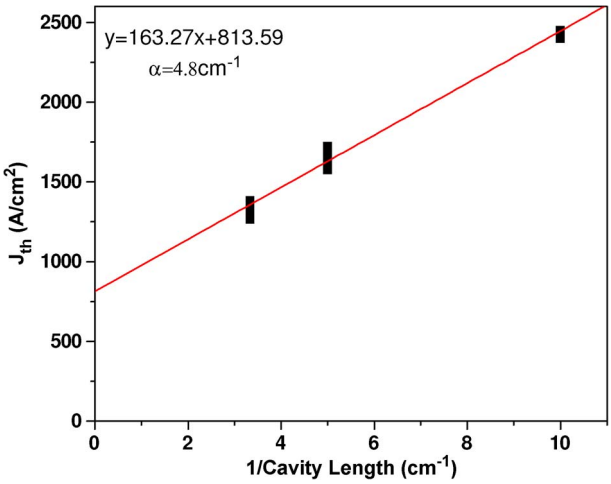

Fig. 9. J_{th} versus 1/Cavity length @RT for six cascade ICL with reduced losses in the hole-injector.

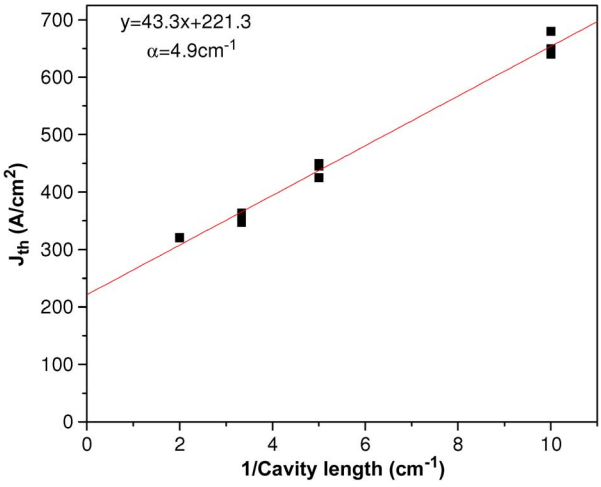

Fig. 10. J_{th} versus 1/Cavity length @RT for a five-cascade ICL with reduced width electron injector.

7. Room-Temperature Operation in a Five-Cascade ICL With a Reduced Electron Injector Length to Increase the Optical Confinement

A five-cascade, n-doped SCR, ICL was grown with a reduced size electron-injector. The width of the electron-injector was reduced from 53 nm to 25 nm for each stage. Ten-micrometer-wide ridge lasers of length 1, 2, 3, and 5 mm were used for a J_{th} versus $1/L_{cav}$ analysis. The results are shown in Fig. 10.

An internal loss of 4.9 cm^{-1} is extracted. By reducing the length of the electron injector, a significant reduction of the slope and of the intercept is obtained. From a least square fit, we extract an uncertainty of 1.5% on both the slope and the intercept. This indicates that much lower threshold current densities are now achievable. This also directly implies that much higher cw temperature operation is possible. A 3 mm long device was high reflectivity (HR) and low reflectivity (AR) coated leading to emission from only the front facet. The $L-I$ characteristics of the device operating at room temperature are shown in Fig. 11. A cw power of 42 mW was measured at room-temperature ($T = 20\ ^{\circ}C$). A threshold current density as low as 367 A/cm^2 was obtained in 3-mm-long devices, which compares with the best ICLs operated CW at room temperature.

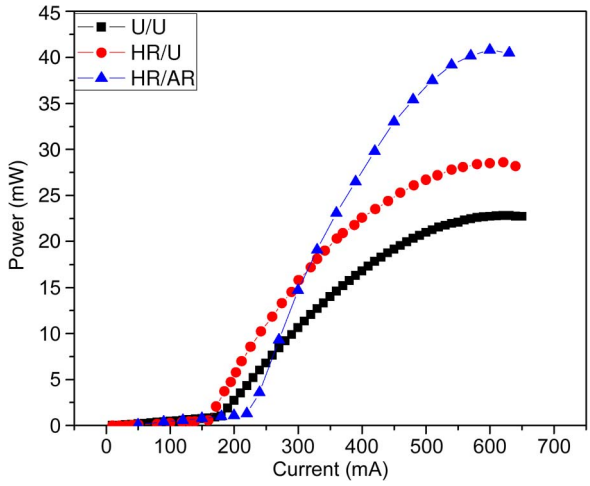

Fig. 11. Three-mm-long, 13-μm ridge, ICL operating at room-temperature ($T = 20\ ^{\circ}\mathrm{C}$).

8. Discussion and Conclusion

This study has elucidated the role of gain and absorption in ICLs. We now have a better understanding of how gain and losses change as we vary the number of stages in an ICL. We have found that the internal losses in ICLs can be reduced to a record low value of $4.8 \pm 0.2\ \mathrm{cm}^{-1}$. We have also found that the internal quantum efficiency per stage can be as high as 86%, as measured at 240 K. Room-temperature operation was obtained in a five-cascade ICL with a reduced width electron injector region. A CW power from the front facet of 42 mW was obtained. Higher power can potentially be obtained from longer devices. From our studies, it is clear that lower threshold ICLs can also be realized by further increasing the modal gain in these lasers. We are presently studying the possibility of increasing the number of wells per stage in the active region. This will increase the differential gain, while also increasing the confinement factor. By doing this, we expect to obtain lower threshold current densities and, very importantly, to reduce the Auger recombination rate. Our studies also indicate that the internal loss coefficient in ICLs is mostly temperature independent over the temperature range from 240 to 281 K.

References

[1] C. L. Canedy, W. W. Bewley, J. R. Lindle, J. A. Nolde, D. C. Larrabee, C. S. Kim, M. Kim, I. Vurgaftman, and J. R. Meyer, "Interband cascade lasers with wavelengths spanning 2.9 μm to 5.2 μm," *J. Electron. Mater.*, vol. 37, p. 1780, 2008.
[2] I. Vurgaftman, C. L. Canedy, C. S. Kim, M. Kim, W. W. Bewley, J. R. Lindle, J. Abell, and J. R. Meyer, "Mid-infrared interband cascade lasers operating at ambient temperatures," *New J. Phys.*, vol. 11, p. 125015, 2009.
[3] W. W. Bewley, J. R. Lindle, C. S. Kim, M. Kim, C. L. Canedy, I. Vurgaftman, and J. R. Meyer, "Lifetimes and Auger coefficients in type-II W interband cascade lasers," *Appl. Phys. Lett.*, vol. 93, no. 4, p. 041118, Jul. 2008.
[4] W. W. Bewley, J. R. Lindle, C. L. Canedy, M. Kim, C. S. Kim, D. C. Larrabee, I. Vurgaftman, and J. R. Meyer, "Gain, Loss, and internal efficiency in interband cascade lasers emitting at $\lambda = 3.6$–4.1 um," *J. Appl. Phys.*, vol. 103, no. 1, p. 013114, Jan. 2008.
[5] C. H. Grein, M. E. Flatte, J. T. Olesberg, S. A. Anson, L. Zhang, and T. F. Boggess, "Auger recombination in narrow-gap semiconductor superlattices incorporating antimony," *J. Appl. Phys.*, vol. 92, no. 12, pp. 7311–7316, Dec. 2002.
[6] M. Kim, C. L. Canedy, W. W. Bewley, C. S. Kim, J. R. Lindle, J. Abell, I. Vurgaftman, and J. R. Meyer, "Interband cascade laser emitting at $\lambda = 3.75$ um in continuous wave above room temperature," *Appl. Phys. Let.*, vol. 92, no. 19, p. 191110, May 2008.
[7] W. Bewley, C. Canedy, C. S. Kim, M. Kim, J. R. Lindle, J. Abell, I. Vurgaftman, and J. Meyer, "Ridge-width dependence of midinfrared interband cascade laser characteristics," *Opt. Eng.*, vol. 49, no. 11, p. 111116, Nov. 2010.
[8] P. M. Smowton and P. Blood, "The differential efficiency of quantum-well lasers," *IEEE J. Sel. Topics Quantum Electron.*, vol. 3, no. 2, pp. 491–498, Apr. 1997.
[9] A. Soibel, K. Mansour, Y. Qiu, C. J. Hill, and R. Q. Yang, "Optical gain, loss, and transparency current in high performance mid-infrared interband cascade lasers," *J. Appl. Phys.*, vol. 101, no. 9, p. 093104, May 2007.

[10] B. A. Ikyo, I. P. Marko, A. R. Adams, S. J. Sweeney, C. L. Canedy, I. Vurgaftman, C. S. Kim, M. Kim, W. W. Bewley, and J. R. Meyer, "Temperature dependence of 4.1 μm mid-infrared type II "W" interband cascade lasers," *Appl. Phys. Lett.*, vol. 99, no. 2, p. 021102, Jul. 2011.
[11] A. Chandola, R. Pino, and P. S. Dutta, "Below bandgap optical absorption in tellurium-doped GaSb," *Semicond. Sci. Technol.*, vol. 20, no. 8, p. 886, Aug. 2005.
[12] J. L. Bradshaw, N. P. Breznay, J. D. Bruno, J. M. Gomes, J. T. Pham, F. J. Towner, D. E. Wortman, R. L. Tober, C. J. Monroy, and K. A. Olver, "Recent progress in the development of type II interband cascade lasers," *Phys. E, Low-Dimensional Syst. Nanostruct.*, vol. 20, no. 3/4, pp. 479–485, Jan. 2004.